

# Bergenin Alleviates Myocardial Ischemia/Reperfusion Injury via Regulating SIRT1 Through Ferroptosis

Lingmei Jia<sup>1,\*</sup>, Siqi Yang<sup>1,\*</sup>, Jun Yin<sup>2</sup>, Ouhua Feng<sup>2</sup>, Zhigang Wang<sup>1</sup>, Min Jia<sup>1</sup>

<sup>1</sup>Cardiovascular Medicine Department, The Second Hospital of Hebei Medical University, Shijiazhuang, People's Republic of China; <sup>2</sup>Cardiovascular Medicine Department, Jingxing County Hospital, Shijiazhuang, People's Republic of China

\*These authors contributed equally to this work

Correspondence: Min Jia; Zhigang Wang, Cardiovascular Medicine Department, The Second Hospital of Hebei Medical University, Shijiazhuang, People's Republic of China, Tel +86-13732219367; +86-15131127511, Email jiamin10086@163.com; 15131127511@163.com

**Objective:** This study aimed to investigate the protective effect of bergenin on myocardial ischemia/reperfusion (I/R) injury and to elucidate its underlying mechanism.

**Methods:** The in vivo model of myocardial I/R injury was established by transient ligation of the left anterior descending coronary artery in Sprague-Dawley rats, which were divided into sham, I/R, I/R+bergenin, and I/R+bergenin+erastin (an agonist of ferroptosis) groups. After the model was established, the rats underwent echocardiography to assess the cardiac function. Hematoxylin and eosin (HE) staining and Masson's trichrome staining were performed to evaluate the cardiac pathological damage. Malondialdehyde (MDA), reactive oxygen species (ROS), glutathione (GSH) and iron levels were measured to determine the ferroptosis level. Western blotting was used to detect the expression of related proteins. Next, H9C2 cells were subjected to oxygen-glucose deprivation/reoxygenation (OGD/R) to mimic the in vitro model of myocardial I/R injury. EX527, a SIRT1 inhibitor, was used to further explore the role of SIRT1 in the myocardial protection of bergenin. In this part of the experiment, H9C2 cells were divided into four groups: control, OGD/R, OGD/R+bergenin, and OGD/R+bergenin+EX527.

**Results:** In vivo experiments, we found that the I/R group showed obvious myocardial pathological damage, oxidative stress and ferroptosis, while the bergenin pretreatment group reversed the above myocardial injury, but this protective effect was inhibited by the ferroptosis inducer erastin. In vitro experiments, compared with the OGD/R group, the bergenin group reduced the oxidative stress level, mitochondrial dysfunction and ferroptosis of H9C2 cells. We found that the protective effect of bergenin on the myocardium was abrogated by EX527. Moreover, Western blotting showed that bergenin activated SIRT1, and increased the phosphorylation of AMPK and the expression level of PGC-1 $\alpha$ .

**Conclusion:** Bergenin exerted a protective effect on the myocardium by modulating the ferroptosis process during myocardial I/R injury through the SIRT1/AMPK/PGC-1 $\alpha$  pathway.

**Keywords:** myocardial ischemia-reperfusion injury1, Bergenin2, ferroptosis3, SIRT14, AMPK5

## Introduction

In the past decade, the number of deaths due to ischemic heart disease has increased by 22.3% worldwide.<sup>1</sup> Currently, thrombolysis and percutaneous coronary intervention are the major strategies to restore blood flow in acute myocardial infarction.<sup>2</sup> However, clinical observations have revealed that some patients experience aggravated symptoms of myocardial ischemia and even extensive necrosis during reperfusion after myocardial ischemia, which is known as myocardial ischemia-reperfusion injury.<sup>3,4</sup> Therefore, how to rapidly rescue the ischemic tissue and mitigate the occurrence of I/R injury at the same time is an urgent challenge in clinical medicine.

Ferroptosis is a genetically, biochemically, and morphologically distinct form of regulated cell death driven by enhanced lipid peroxidation and insufficient capacity to eliminate hydroperoxy-lipids.<sup>5</sup> Iron is the central to the execution

of the Ferroptosis program.<sup>6</sup> Acyl-coa synthetase long-chain family member 4 (ACSL4) and glutathione peroxidase 4 (GPX4) regulate polyunsaturated fatty acids (PUFAs) metabolism and glutathione (GSH) biosynthesis, respectively.<sup>7,8</sup> Solute carrier family 7 member 11 (SLC7A11) is an important component of cystine/glutamate transporters, which can regulate cellular lipid peroxidation and inhibit iron accumulation.<sup>9</sup> These proteins play an important role in modulating the biological behavior of ferroptosis. It has been reported that ferroptosis is involved in the pathogenesis of various cardiac diseases such as myocardial infarction, myocardial ischemia-reperfusion,<sup>10</sup> cardiomyopathy,<sup>11,12</sup> and heart failure.<sup>13</sup>

Mitochondrial dysfunction is a key factor in the pathogenesis of myocardial ischemia-reperfusion injury. Silent mating-type information regulator 2 homologue 1 (SIRT1) is a nicotinamide adenine dinucleotide-dependent histone deacetylase that can deacetylate various proteins and modulate oxidative stress. Peroxisome proliferator-activated receptor- $\gamma$  coactivator 1 $\alpha$  (PGC-1 $\alpha$ ) is a deacetylation target of SIRT1. Activation of SIRT1 can enhance the expression of PGC-1 $\alpha$ , thus attenuating oxidative stress injury. Adenosine 5'-monophosphate (AMP)-activated protein kinase (AMPK) is an AMP-dependent protein kinase and a classical downstream effector of the SIRT1 signaling pathway. As a vital kinase that regulates energy homeostasis, it mainly monitors the cellular energy input and output and maintains the normal physiological functions of cells. AMPK can ameliorate mitochondrial dysfunction and promote cell survival via PGC-1 $\alpha$ . Therefore, it is hypothesized that the SIRT1/AMPK/PGC-1 $\alpha$  signaling pathway plays a crucial role in protecting against oxidative stress and mitochondrial dysfunction.

Bergenin is a compound extracted from various medicinal plants, which exhibits anti-inflammatory, anti-tumor, and anti-oxidant effects. As a natural plant-derived product, it has abundant sources, low cost, and promising development potential. Regarding its role in counteracting different pathological conditions, bergenin is a potent antioxidant. Moreover, it reduces the oxidative damage and lipid peroxidation induced by ischemia-reperfusion both in vivo and in vitro.<sup>14–16</sup> This may activate the antioxidant system through a SIRT1-mediated mechanism. Therefore, whether bergenin regulates ferroptosis through the SIRT1/AMPK/PGC-1 $\alpha$  signaling pathway to exert a protective effect on myocardial ischemia-reperfusion injury requires further investigation.

## Materials and Methods

### Materials

Bergenin and Erastin were purchased from Meilun Biochemical Technology (Liaoning, China). Sirt1-specific inhibitor EX527 was purchased from MCE (Shanghai, China). The drug was dissolved in DMSO and diluted to the desired concentration with 0.9% saline.

### Experimental Animals and MI/R Models

All animal procedures were performed in accordance with the National Institutes of Health Guide for the Care and Use of Laboratory Animals (NIH Publication No. 86–23,1996). It was approved by the Experimental Animal Research Committee of Hebei Medical University. Male SD rats (8-week-old, 280–300g) were from the Animal Center of Hebei Medical University, and the animals were kept in cages with a 12-hour light/dark cycle for 1 week before the experiment. The rats ate and drank freely.

Eight-week-old male SD rats were randomly selected and divided into sham group, IR group, IR+bergenin group, and IR+bergenin+Erastin group. Before surgery, bergenin solvent (250 mg/kg/d) was administered to the rat by gavage every other day for 3 days. Erastin (80mg/kg/d, i.p.) was administered once daily for 3 consecutive days before IR. The Sham group was intraperitoneally injected with the same dose of normal saline as the IR group.

Before surgery, the rats were fasted for 12 h, anesthetized by intraperitoneal injection of pentobarbital sodium (45 mg/kg), and then intubated and connected to a small animal ventilator for positive pressure ventilation. Then, the skin was prepared, sterilized, and the skin was dissected longitudinally for about 2cm along the mid-clavicular line. The subcutaneous tissue and muscle were separated layer by layer with hemostatic forceps in the third or fourth intercostal area. The chest was opened through sternotomy, and the left anterior descending coronary artery was exposed. Next, a 6.0 suture was threaded below the LAD coronary artery approximately 2 mm from the lower margin of the left atrial

appendage. Subsequently, a 6.0 suture sliding ring with 1 to 2 mm diameter was placed around the LAD and the ligation was tightened to occlude the artery. We successfully established the AMI/R model when the ST segment in lead II of the ECG was elevated and the myocardial surface of the ligated area was observed to become pale. The chest wall was then sutured with 5–0 black medical sutures, and after 30 min of ischemia, the sliding ring was removed to restore blood flow. After 12 hours of reperfusion, mechanical ventilation was stopped after the heart rate and respiration were stable. The sham group underwent myocardial exposure after thoracotomy but no LAD ligation.

## Cell Culture and Protocol

H9c2 cells were obtained from Fuhang Chemical Technology Co., Ltd. (Shanghai, China) and cultured in Du-type modified Eagle medium (DMEM containing 10% fetal bovine serum), 100U/mL penicillin and 0.1mg/mL streptomycin in a humidified cell incubator (95% air, 5%CO<sub>2</sub>) at 37 ° C. MI/R of cardiomyocytes in vitro was simulated by 12 h hypoxia followed by 2 h reoxygenation. During hypoxia, serum-free and glucose-free media were replaced to establish an oxygen-glucose deprivation (OGD/R) model.

The cells were treated with 1μM, 10μM, 25μM, 50μM, 100μM and 1mM bergenin during hypoxia and reoxygenation, respectively. The SIRT1-specific inhibitor EX527 at a concentration of 10μM was added during both hypoxia and reoxygenation. H9c2 cells were divided into four groups: control group, OGD/R group, OGD/R+ Bergenin group and OGD/R+ Bergenin +EX527 group.

## HE Staining

Three days after I/R, the rat were anesthetized again. The chest was opened. The hearts were exposed. Blood vessels, fat, pericardium, and heart chambers were quickly removed. First, the heart tissue was fixed in 4% formaldehyde (overnight, 4°C). Secondly, the sample tissues were gradually dehydrated, transparent and embedded in paraffin in different alcohol concentrations. Wax blocks with embedded tissue were removed and sectioned at a thickness of 4–6 μm. The paraffin was then removed with xylene, and the sections were stained in an aqueous solution of hematoxylin for several minutes, observing the color every few seconds, rinsed with water for 1 hour, and placed in distilled water for some time. After 2 to 3min of staining with eosin stain solution, the cells were dehydrated with absolute ethanol. Finally, the sections were made transparent with xylene and inspected for mounting. The staining effect was observed under an inverted microscope, and the histopathological changes were observed under 100× and 200 × field of view.

## TTC Staining

Following euthanasia by anesthetic overdose, the heart was rapidly excised (within 5 min) and immersed in 0–4°C saline solution. The heart was then frozen at –20°C for 1 hour. Transverse sections of the heart, 2 mm thick, were incubated in 2% tetrazolium chloride solution (Beijing solarbio Science Technology Co.,Ltd G3005) for 15 min at 37°C in the dark. The sections were rinsed with PBS solution for 3–5 min and fixed with 10% neutral formaldehyde for 6 h. Photographs of the sections were taken and analyzed using ImageJ software. The infarct area and total area of each section were measured. The infarct volume of each section was calculated as the product of the infarct area and the section thickness. The total infarct volume was obtained by summing up the infarct volumes of all sections.

## Masson's Trichrome Staining

Paraffin-embedded sections were deparaffinized in xylene and rehydrated in graded ethanol. The sections were stained with Weigert's iron hematoxylin for 5 min, washed with tap water, differentiated with 1% hydrochloric acid in 70% ethanol for a few seconds, and rinsed with tap water and running water for several minutes. The sections were then stained with ponceau-acid fuchsin solution for 5–10 min, rinsed briefly with distilled water, and treated with phosphotungstic/phosphomolybdic acid solution for 3–5 min. The sections were counterstained with aniline blue solution for 5 min, differentiated with 1% acetic acid for 1 min, and dehydrated in graded ethanol. The sections were cleared in xylene, air-dried, and mounted with neutral balsam. The sections were examined under a light microscope, and images were captured and analyzed.

## Cardiac Echocardiography

Small animal echocardiography was performed 3 days after surgery. Anesthesia: Intraperitoneal injection of pentobarbital sodium 50 mg/kg. The rats were laid flat on a heating plate at 37 ° C. Set the ultrasonic parameters of high frequency color ultrasonic instrument for small animals: Heart Rate (HR), Left ventricular ejection fraction (LVEF), Left ventricular fractional shortening (LVFS).

## Reactive Oxygen Species Assay Kit - High Sensitivity DCFH-DA

Intracellular ROS levels were detected by DCFH-DA (Solarbio, China) fluorescence. After culturing and washing with PBS three times in 6-well plates, H9c2 cells were incubated in the dark with 10uM DCFH DA for 30 min at room temperature. Photographs were taken using a fluorescence microscope at an excitation/emission wavelength of 504/529nm. Green fluorescence intensity was analyzed by image J software.

## Detection of MDA, an Oxidative Damage Assessment Index

The detection kit was used to detect malondialdehyde (MDA)(Nanjing Jiancheng Bioengineering Institute A003-1-2), the tissue and cells were operated according to the manual, and the OD value was measured at 532nm of the microplate reader.

## The Measurement of Fe<sup>2+</sup> Content

Cell Ferrous Iron Colorimetric Assay Kit (Elabscience E-BC-K881-M) was used for the measurement of Fe<sup>2+</sup> content. 5 µL detection buffers and 100 µL iron probes were added to the test samples in turn, and they were mixed well and detected at 37 °C Incubate in dark for 60 min at room temperature. The OD value was detected at 593 nm.

## Determination of Mitochondrial Membrane Potential (MMP)

MMP is an important indicator to evaluate mitochondrial function. Changes in mitochondrial membrane potential were analyzed by JC-1 staining (Beijing solarbio Science Technology Co.,Ltd Cat#M8650). H9c2 cells were treated in groups, stained with 10µM JC-1 for 30 min at room temperature in the dark, and observed by fluorescence microscope. The ratio of red/green fluorescence was calculated by Image-J to detect mitochondrial function.

## Determination of Glutathione and Superoxide Dismutase

GSH and SOD (Nanjing Jiancheng Bioengineering Institute A061-1-2 and A001-3-2) are important components in the antioxidant system. The tissues and cells were operated according to the reagent instructions respectively, and the OD values of GSH and SOD were measured at 520nm and 450nm respectively with a microplate reader.

## Western Blot Analysis

Western blot detection SIRT1, PGC - 1 alpha, GPX4, XCT, FTH1, ACSL4, AMPK, the expression of P - AMPK. GAPDH was used as a control. In brief, proteins were extracted by RIPA buffer (Solarbio R0010) and quantified using a BCA kit (Solarbio PC0020). Subsequently, 30µg of protein was loaded onto 10% SDS-PAGE, transferred to PVDF membranes, and then blocked in 5% nonfat milk. The membranes were incubated with primary antibody sirt1 (ZENBIO, mAb:R25721 1:1000), pgc1α (ZENBIO, 1:1000), ampk (ZENBIO, 1:500), p-ampk (ZENBIO, 1:500), Anti-gpx4 antibody (ZENBIO cat no.381958 1:1000), anti-XCT antibody (ZENBIO,pAb:382036, 1:1000) and anti-GAPDH antibody (ZENBIO,cat no.380626, 1: 10000) were incubated overnight at 4°C, followed by incubation with the corresponding horseradish peroxidase labeled anti-rabbit IgG antibody (ZENBIO,cat no.511203,1:1,0000) for 1 h at room temperature. The films were scanned by enhanced chemiluminescence (ECL). Finally, image J software was used for analysis.

## Terminal-Deoxynucleotidyl Transferase Mediated Nick End Labeling (TUNEL)

According to the instructions of the TUNEL Apoptosis Detection Kit (Green Fluorescence, Abbkine,KTA2010), the tissue sections were fluorescently stained deoxyribonucleotide terminal transferase, based on the notch end labeling method. The tissue sections were deparaffinized and dehydrated, incubated with proteinase K for 15 minutes, and



incubated with TUNEL staining reagent at 37 °C for 1 hour in the dark. Photographs were taken using a fluorescence microscope at an excitation/emission wavelength of 490nm/520 nm.

## Statistics

All experiments were repeated at least three times and a representative result is presented. All experimental data are presented as mean  $\pm$  standard deviation. *t* test (two-sided) was used for comparison between the two groups. One-way ANOVA and Tukey post hoc test were used for multiple comparisons. SPSS 26.0 (SPSS, Inc) was used for statistical processing.  $P < 0.05$  was considered statistically significant.

## Result

### Result I: Bergenin Attenuates Cardiac Injury in IR Rats

To explore the protective effects and mechanisms of Bergenin on ischemia-reperfusion (IR) rats, we established a rat model of myocardial IR by transiently occluding the left anterior descending coronary artery, and randomly assigned the rats to four groups: sham group, IR group, IR+Bergenin group, IR+Bergenin+erastin group (a potent ferroptosis inducer). We performed TTC staining on the hearts of each group, and observed that the Bergenin group had a smaller myocardial infarction area than IR group (Figure 1A and B). We assessed the cardiac function of IR rats by echocardiography, and obtained the M-mode images of the left ventricular short axis. We found that compared with the sham group, the left ventricular ejection fraction (LVEF) and fractional shortening (FS) of the IR group were significantly reduced, indicating that the cardiac contractility was compromised. Compared with the IR group, the LVEF and FS of the Bergenin group were enhanced, indicating that Bergenin could improve the cardiac function of IR rats (Figure 1C–E). The above

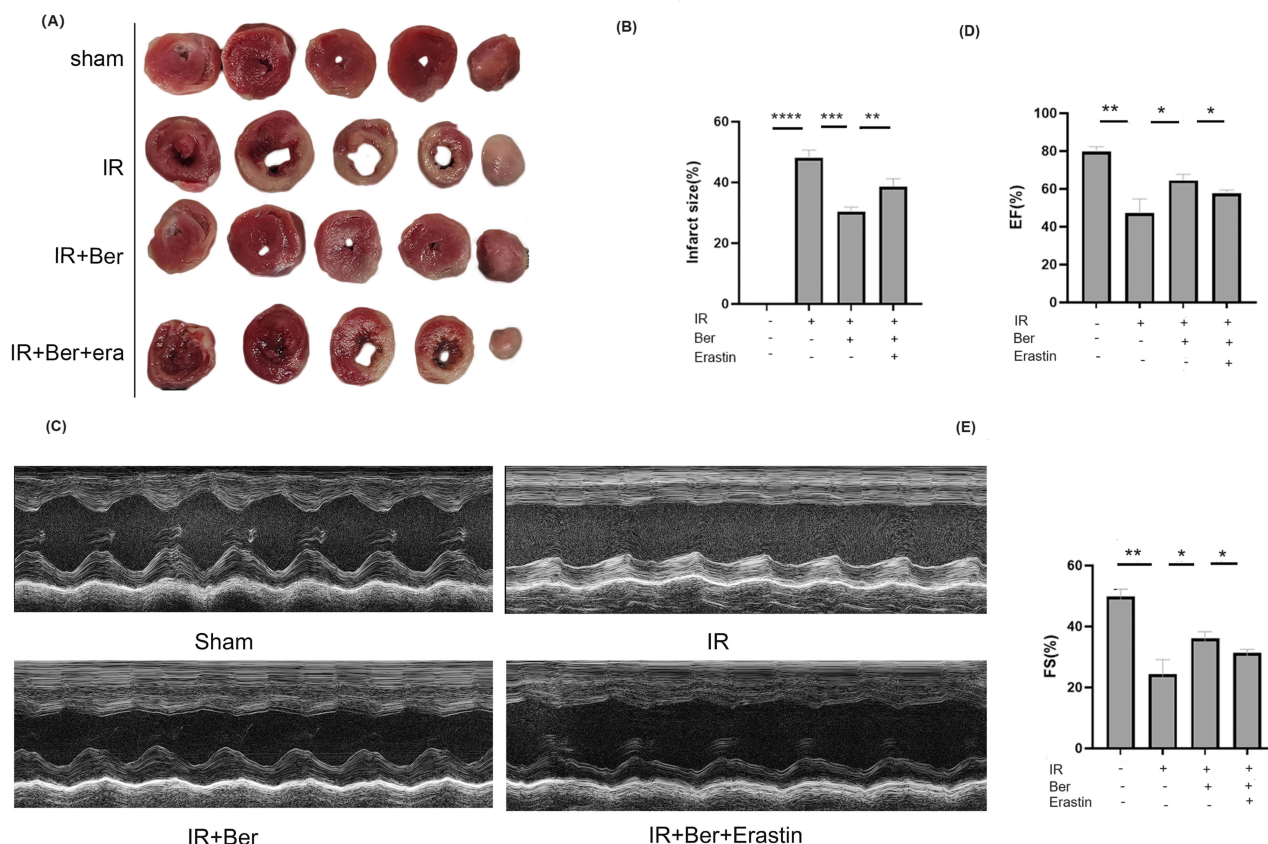


**Figure 1** Treatment with bergenin mitigated myocardial infarction and preserved cardiac function in I/R rat. 24 hrs post I/R, infarct size (A and B) was assayed by TTC staining. Myocardial function was assayed by M-mode echocardiography. Representative echocardiographic images (C) and EF (D) and FS (E) were shown. The data are presented as the mean  $\pm$  SD,  $n=3-5$ . \* $p < 0.05$ , \*\* $p < 0.01$ , \*\*\* $p < 0.001$  and \*\*\*\* $p < 0.0001$ .

protective effects of Bergenin were abrogated by erastin, suggesting that Bergenin ameliorated the cardiac functional impairment induced by myocardial IR via ferroptosis.

## Result 2: Bergenin Mitigates Myocardial Histopathological Damage and Apoptosis in IR Rats

To examine the histopathological alterations of cardiac tissue in IR rats, we embedded the myocardial tissue in paraffin and performed hematoxylin and eosin (HE) staining (Figure 2A). We noticed that the IR group exhibited myocardial cell hypertrophy, disorganized and sparse myocardial fibers, loss of normal architecture, interstitial edema, myocardial fiber disruption and inflammatory cell infiltration, marked changes of contraction bands and extensive erythrocyte extravasation, while the administration of Bergenin ameliorated the above alterations. Masson's trichrome staining (Figure 2B) revealed that compared with the sham group, the IR group had abundant collagen deposition, while the administration of Bergenin diminished the collagen deposition. The addition of erastin increased ferroptosis, which abolished the above protective effects of Bergenin, further indicating that Bergenin attenuated the myocardial injury elicited by ischemia-reperfusion via ferroptosis. We conducted terminal deoxynucleotidyl transferase-mediated dUTP nick end labeling (TUNEL) staining (Figure 2C and D) on the myocardial tissue, and observed that when the myocardium underwent ischemia-reperfusion, a large number of cells were apoptotic, while the administration of Bergenin reduced the apoptosis rate.

## Result 3: Bergenin Mitigates Ferroptosis in IR Rats

To elucidate whether myocardial ischemia-reperfusion induces ferroptosis and the protective mechanism of Bergenin, we measured the levels of ferroptosis-related proteins. Western blot analysis revealed that compared with the sham group, the IR group exhibited the reduction in GPX4, XCT, and FTH1 (Figure 3A–E). However, the administration of Bergenin restored the expression of the above ferroptosis-related proteins. Moreover, we found that Bergenin could suppress the elevation of MDA and augment the expression of SOD and GSH during myocardial ischemia-reperfusion. This indicates that Bergenin attenuates ferroptosis in IR rats.

## Result 4: Bergenin Improves Cell Survival of H9C2 Cells During OGD/R

To investigate the cytotoxic effect of Bergenin on H9C2 cells, we exposed H9C2 cells to different concentrations of Bergenin (12.5UM, 25UM, 50UM, 100UM, 1MM), and the CCK8 assay results demonstrated that Bergenin was not cytotoxic (Figure 4A). Next, we applied different concentrations of Bergenin (12.5UM, 25UM, 50UM, 100UM, 1MM) before OGD/R in H9C2 cells. The results indicated that compared with the control group, Bergenin enhanced the cell survival of each group, exhibiting a concentration-dependent manner, and the cell survival improvement effect was more prominent in the 100UM concentration group (Figure 4B). Therefore, we selected Bergenin 100UM as the concentration for the following experiments. The cell experiments were categorized into four groups: blank control group NC, OGD/R, OGD/R+Bergenin, OGD/R+Bergenin+EX527 (a SIRT1 inhibitor). The cell survival assay showed that compared with the control group, the cell survival of the OGD/R group was markedly reduced, suggesting that the oxygen-glucose deprivation model was successfully established (Figure 4C). Compared with the OGD/R group, the cell survival of the OGD/R+Bergenin group was elevated, suggesting that Bergenin improved the cell survival of H9C2 cells during OGD/R.

## Result 5: Bergenin Protects Against Mitochondrial Dysfunction and Apoptosis in H9C2 Cells Subjected to OGD/R

Mitochondrial membrane potential (MMP) is a marker of mitochondrial and cellular activity. Mitochondrial JC-1 aggregates emit red fluorescence, while JC-1 monomers emit green fluorescence (Figure 5A and B). The ratio of red to green fluorescence reflects the changes of MMP, indicating the mitochondrial function status. The results showed that MMP decreased during OGD/R, while Bergenin restored the mitochondrial function. Moreover, as we expected, EX527 antagonized the protective effect of Bergenin on mitochondrial function. In conclusion, we propose that Bergenin exerts its protective effect on mitochondria of H9C2 cells subjected to OGD/R via SIRT1. In addition, the cell apoptosis assay

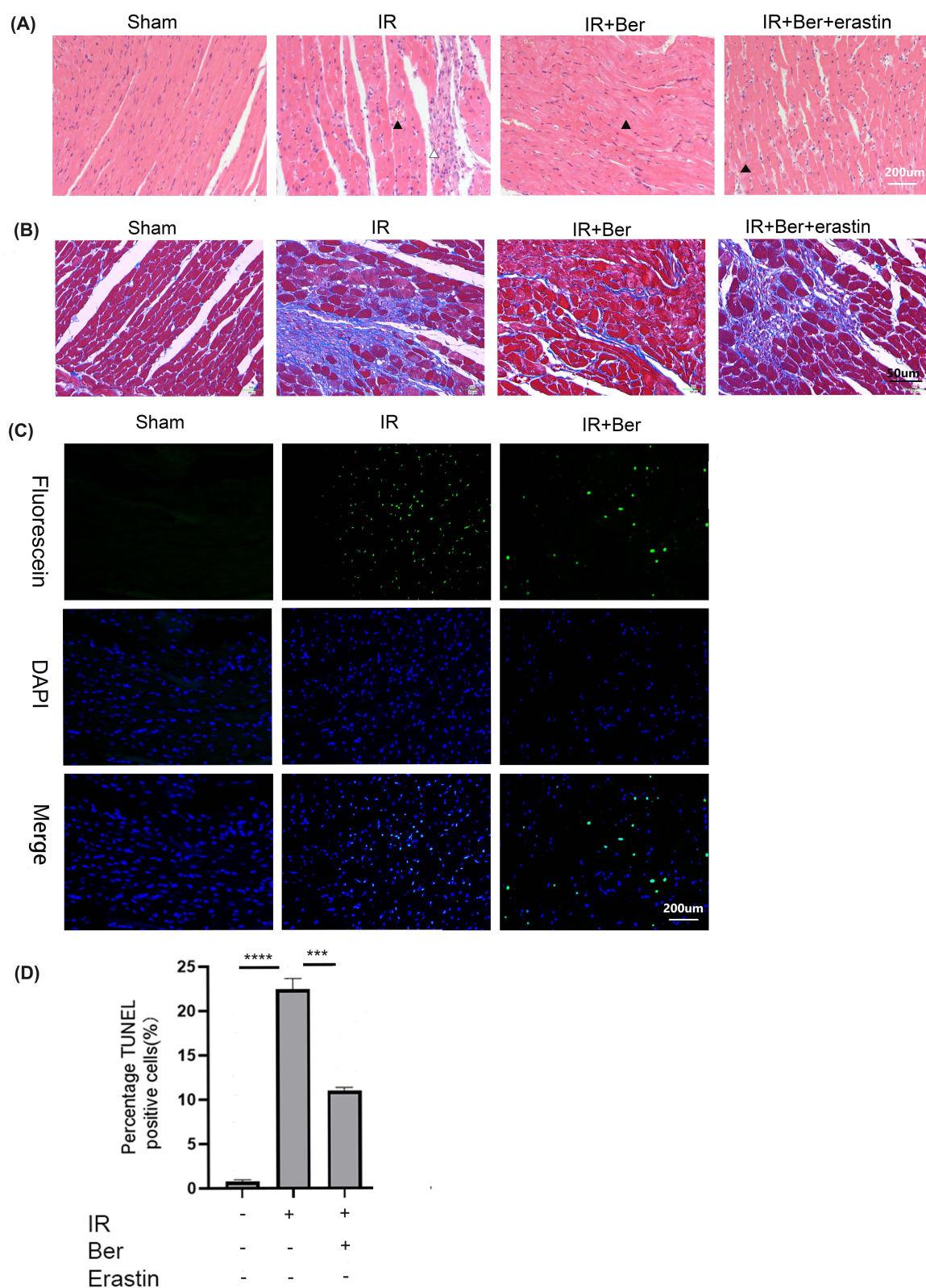


**Figure 2** Representative images (200×) showing HE staining. Pathological changes show extensive extravasation of red blood cells (first black triangle), inflammatory reaction (white triangle), thinning and wavy myofibrils (second black triangle) and extensive contraction band change (third black triangle) (A); Masson's trichrome staining (400X) was used to examine myocardial tissue's pathological and morphological changes. Blue: collagen fibers; Red: muscle fibers (B); Representative fluorescent images of TUNEL (C); The quantification of the TUNEL fluorescence intensity (200X) (D). The data are presented as the mean ± SD, n=3-5. \*\*\*\*p<0.0001 and \*\*\*p<0.001.

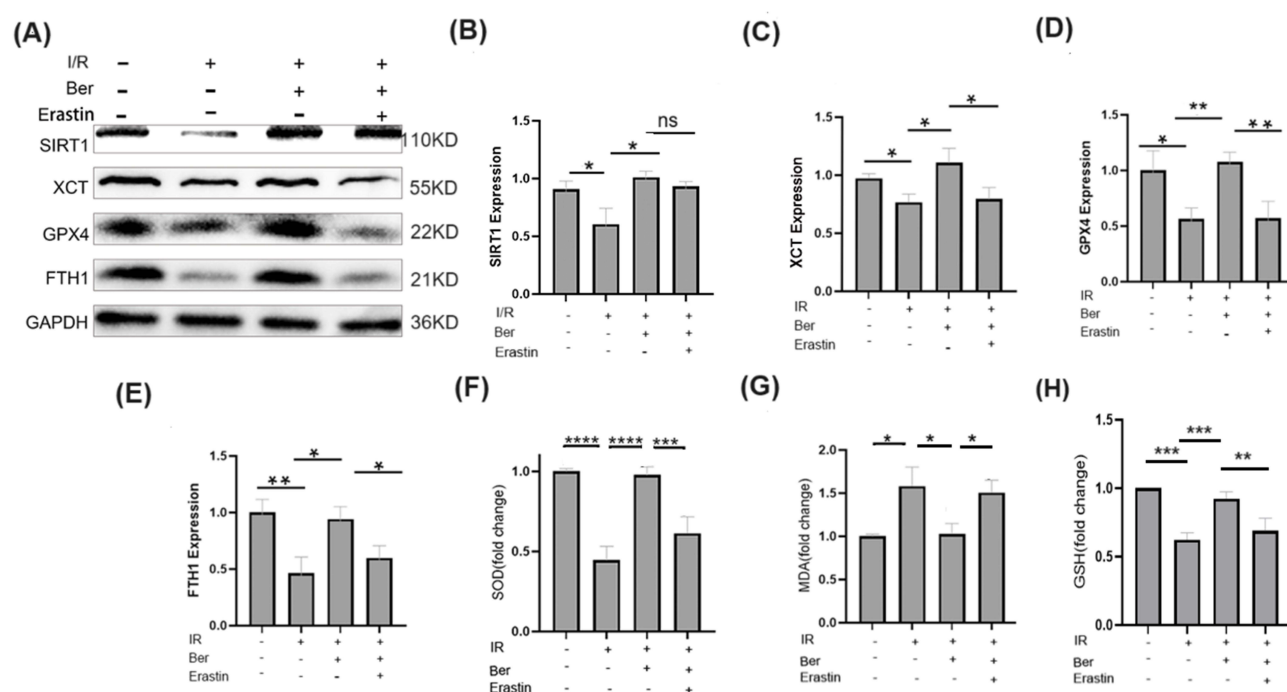


**Figure 3** Sirt1 is an important anti-ferroptosis factor: Western blot detected the expression of related proteins (A). The quantification of the expression of related proteins (B–E). GSH (F), SOD (G), and MDA (H) expression in rat of myocardial ischemia-reperfusion. The data are presented as the mean $\pm$ SD, n=3–5. ns no statistically significant. \*p<0.05, \*\*p<0.01, \*\*\*p<0.001 and \*\*\*\*p<0.0001.

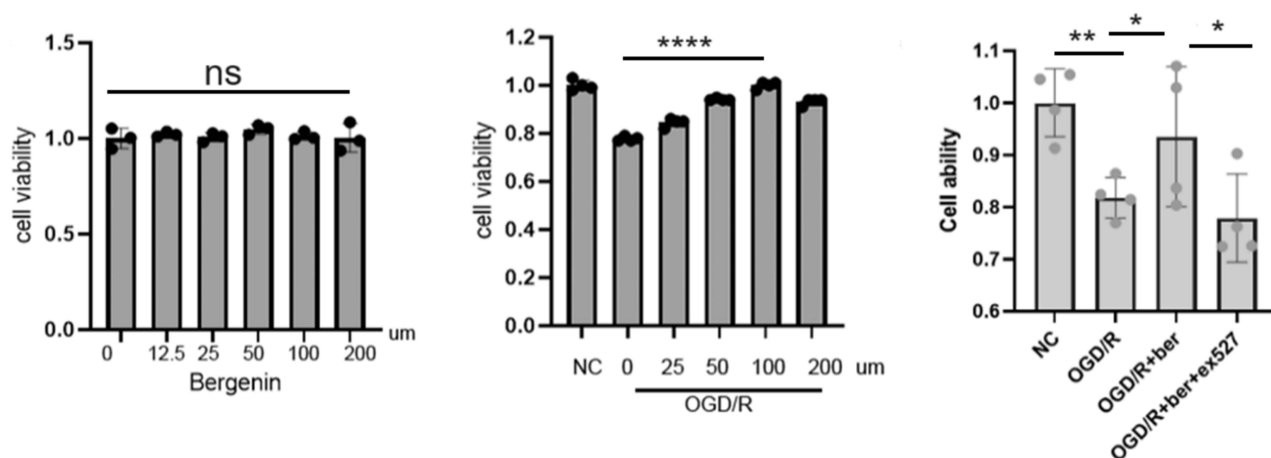


**Figure 4** Cell viability under different experimental conditions. (A–C) The data are presented as the mean $\pm$ SD, n=3–5. ns no statistically significant., \*p<0.05, \*\*p<0.01 and \*\*\*p<0.0001.

showed that Bergenin attenuated the OGD/R injury (Figure 5C and D), but this effect was also abrogated by SIRT1 inhibitor EX527.

## Result 6: Bergenin Prevents Ferroptosis in H9C2 Cells Subjected to OGD/R

We found that compared with the control group, the OGD/R group had significantly elevated levels of ROS (Figure 6A and B) and MDA (Figure 6C), and significantly reduced levels of GSH (Figure 6D) and SOD (Figure 6E). Bergenin reversed these changes. This suggests that Bergenin alleviates the oxidative stress response in H9C2 cells, and EX527 inhibits the effect of Bergenin, implying that the protective effect of Bergenin is mediated by SIRT1. WB results showed that compared with the OGD/R group, bergenin increased the expression of GPX4, XCT, and FTH1 (Figure 6F–I), suggesting that bergenin could



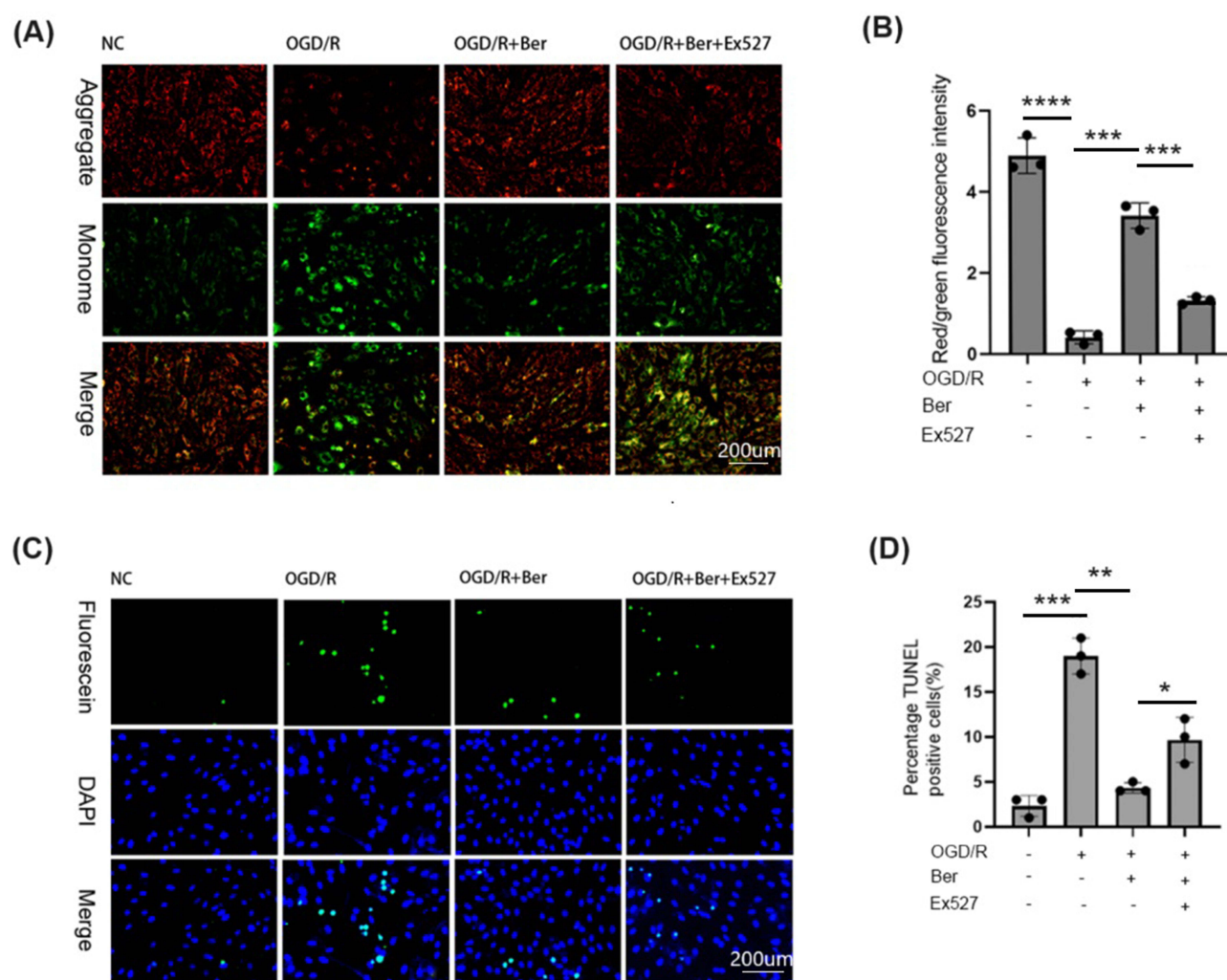


**Figure 5** Bergenin prevents MI/R-induced cardiomyocyte mitochondrial dysfunction and apoptosis. JC-1 fluorescence was observed by fluorescence microscope to detect MMP. Red fluorescence represents the mitochondrial aggregate form of JC-1. Green fluorescence represents the monomeric form of JC-1. (200×) (A). Quantitative analyses of JC-1 fluorescence intensity are shown in the right panel (B). The left panel shows representative images of cardiac tissue stained by TUNEL (green) and DAPI (blue) (200×) (C). Quantitative analyses of TUNEL-positive myocytes are shown in the right panel (D). The data are presented as the mean±SD, n=3–5. \*p<0.05, \*\*p<0.01, \*\*\*p<0.001 and \*\*\*\*p<0.0001.

decrease the ferroptosis level in H9C2 cells, and this effect was also blocked by EX527 (SIRT1 inhibitor). Meanwhile, the iron level showed that iron accumulation occurred in H9C2 cells during OGD/R, bergenin could readjust the iron distribution, lower the intracellular iron (Figure 6J), and attenuate the ferroptosis level, and this effect was also nullified by EX527, suggesting that bergenin prevents ferroptosis in H9C2 cells via SIRT1 pathway.

## Result 7: Bergenin Confers Protection to H9C2 Cells via SIRT1/AMPK/PGC1-α Pathway

SIRT1 is a NADH-dependent deacetylase, and PGC-1α is its canonical downstream substrate. We postulated that SIRT1 might deacetylate PGC-1α in myocardial ischemia-reperfusion. Western blot results revealed that in H9C2 cells exposed to OGD/R injury, SIRT1 was downregulated, p-AMPK was upregulated, and PGC1-α was downregulated (Figure 7A–D). Upon treatment with bergenin, SIRT1 and PGC1-α were upregulated, and p-ampk/AMPK were further upregulated. This indicates that the activation of SIRT1 enhanced the phosphorylation of AMPK and its downstream effector PGC1-α. When EX527 was added, the phosphorylation of AMPK was suppressed, and the expression of its downstream effector PGC1-α was reduced. The results imply that during the hypoxia-reoxygenation process of H9C2 cells, bergenin activated



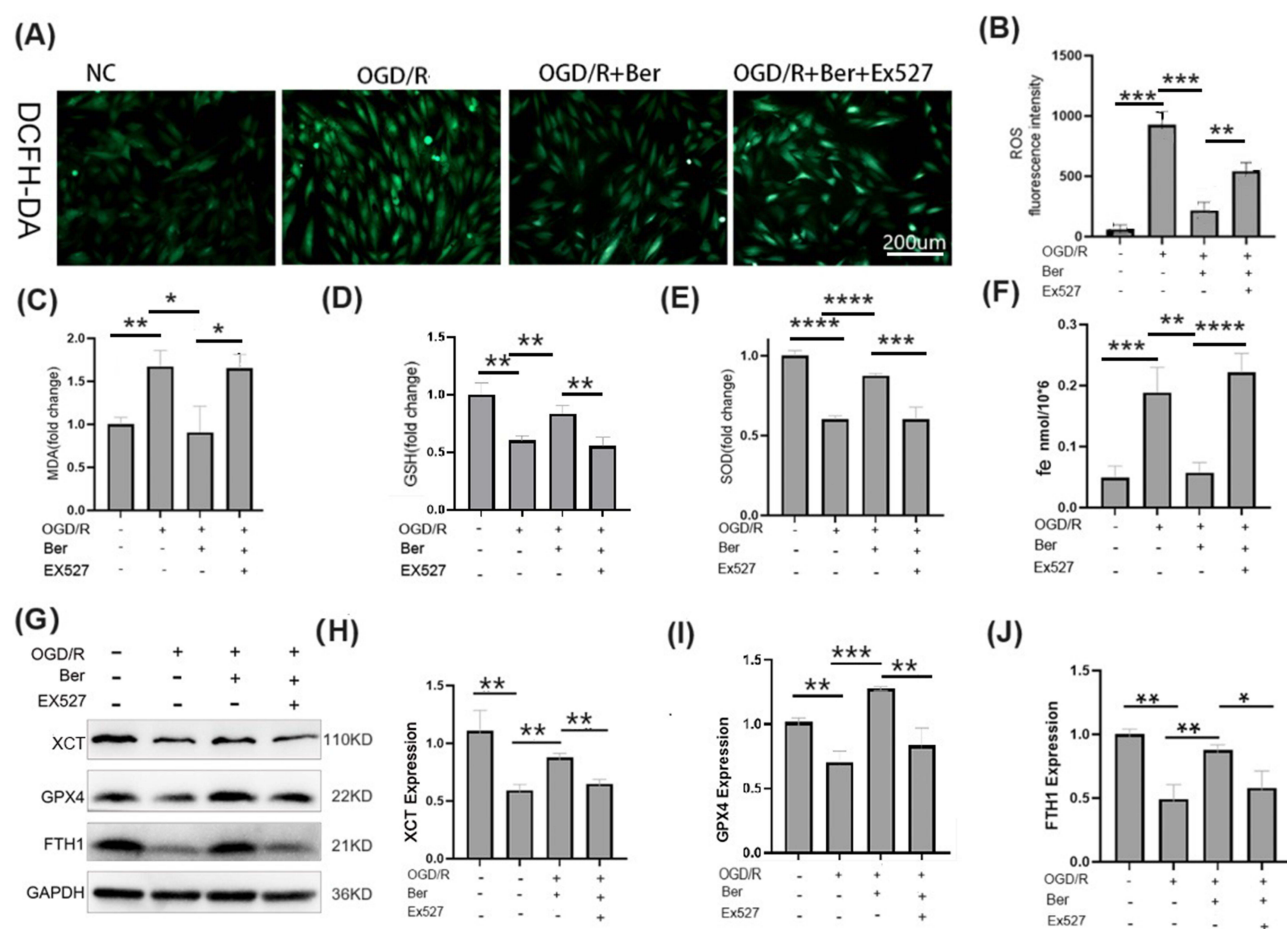


**Figure 6** The panel shows representative images of H9C2 cell stained by dihydroethidium (DHE) to determine ROS content (A). Quantitative analyses of DHE fluorescence intensities are shown on the right (B). MDA (C), GSH (D) and SOD (E) expression in H9C2 cell of OGD/R. Level of Fe<sup>2+</sup> (F) expression in H9C2 cell of OGD/R. Western blot detected the expression of related proteins (G). The quantification of the expression of related proteins (H-J). The data are presented as the mean±SD, n=3-5. \*p<0.05, \*\*p<0.01, \*\*\*p<0.001 and \*\*\*\*p<0.0001.

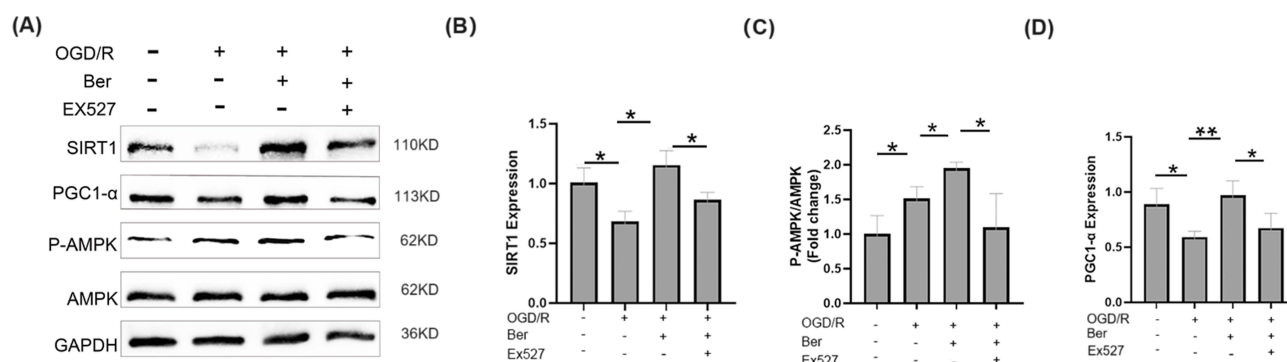


**Figure 7** Western blot detected the expression of related proteins (A). The quantification of the expression of related proteins (B-D). The data are presented as the mean±SD, n=3-5. \*p<0.05, \*\*p<0.01.

SIRT1, and subsequently activated the phosphorylation of AMPK and its downstream effector PGC1-α. Therefore, the protective effect of bergenerin on H9C2 cells might be partly attributed to the upregulation of SIRT1/AMPK/PGC1-α pathway.

## Discussion

So far, there is no effective pharmacological intervention for I/R injury in clinical practice. Therefore, many studies are devoted to finding ways to reduce myocardial ischemia-reperfusion injury. Myocardial ischemia-reperfusion injury is related to multiple pathophysiological pathways, such as oxidative stress, calcium overload, mitochondrial dysfunction, cell apoptosis, autophagy, ferroptosis, etc.<sup>17</sup> In our rat experiment, when myocardial ischemia-reperfusion occurred, the cardiac contractile function was significantly reduced, and the pathological staining suggests that the cardiac tissue had a inflammatory response and structural disorder.

Bergenin is a C-glucoside of 4-O-methyl gallic acid that a natural compound with remarkable anti-inflammatory and antioxidant properties. This study aims to determine the protective effect of bergenin on myocardial I/R injury and explore new signaling pathways, providing a new perspective for the prevention and treatment of myocardial I/R injury. Firstly, we verified in vivo that bergenin attenuated the cardiac function decline and pathological damage mediated by ferroptosis in myocardial ischemia-reperfusion injury. Then we found in vitro that the H9c2 cells in the oxygen-glucose deprivation group activated the ferroptosis and apoptosis pathways, increased the cellular oxidative stress level and mitochondrial dysfunction, while adding bergenin could reduce the ferroptosis level and mitochondrial dysfunction of H9c2 cells and increase cell viability.

Ferroptosis is a mode of cell death caused by the accumulation of intracellular iron and lipid reactive oxygen species (ROS), which plays an important role in the development of various diseases, such as Parkinson's disease, cancer, ischemia-reperfusion injury, etc.<sup>18</sup> The characteristics of ferroptosis include glutathione (GSH) depletion, glutathione peroxidase 4 (GPX4) inactivation, lipid peroxidation accumulation, etc.<sup>18</sup> FTH1 is a key member of iron metabolism, responsible for the storage of Fe<sup>2+</sup>. In H9C2 cardiomyocytes, the oxygen-glucose deprivation model group showed a decrease in XCT, GPX4, and GSH consumption, and an accumulation of ROS and iron ions, which verified the occurrence of ferroptosis in this process. SIRT1 is a NAD<sup>+</sup>-dependent deacetylase, involved in the regulation of various physiological and pathological processes, such as aging, metabolism, inflammation, oxidative stress, etc. In recent years, more and more studies have shown that SIRT1 is closely related to ferroptosis and can affect the occurrence and process of ferroptosis through various mechanisms.

On the one hand, SIRT1 can regulate ferroptosis by modulating iron metabolism. Iron metabolism disorder can lead to an increase in free iron in the cell, and iron can catalyze the production of ROS through the Fenton reaction, and ROS further promote lipid peroxidation, leading to lipid peroxidation accumulation, inducing ferroptosis.<sup>5</sup> SIRT1 can regulate iron metabolism in various ways, such as inhibiting the expression of hepcidin,<sup>4</sup> promoting the synthesis of ferritin,<sup>19</sup> affecting the expression of transferrin receptor, etc., thereby reducing the level of intracellular iron or inhibiting the activity of various iron-containing metalloenzymes that catalyze lipid peroxidation reactions, increasing the resistance to ferroptosis. In our experiment, we found that the oxygen-glucose deprivation model group increased the accumulation of iron, while adding bergenin (SIRT1 activator) reference could reduce the iron concentration, and adding SIRT1 inhibitor EX527, bergenin could no longer reduce the iron ion concentration. This result shows that in the process of myocardial ischemia-reperfusion, the activation of SIRT1 can regulate the iron ion concentration, thereby reducing the occurrence of ferroptosis.

On the other hand, SIRT1 can modulate ferroptosis by regulating the amino acid antioxidant system. Amino acids are crucial for ferroptosis. System xc- is a reverse transport protein that imports cystine into the cell and converts it to cysteine, which is used to produce the main intracellular antioxidant GSH. GSH is a vital cofactor of GPX4, which can restore lipid peroxides to normal lipids, prevent lipid peroxide accumulation, and suppress ferroptosis. SIRT1 can regulate the expression or activity of System xc- and GPX4 directly or indirectly, thereby influencing the synthesis and utilization of GSH, counteracting oxidative stress, and preventing ferroptosis.<sup>20</sup> For instance, SIRT1 can deacetylate p53, inhibit its transcriptional activity, and diminish the inhibitory effect of p53 on System xc;<sup>20</sup> SIRT1 can also deacetylate FOXO3a, activate its transcriptional activity, and enhance the expression of GPX4. Our experiment is in agreement with the previous results. In the oxygen-glucose deprivation model, the expression levels of XCT, GPX4, and GSH all declined, and bergenin, an activator of SIRT1, could reverse these expressions, while after adding EX527, bergenin could not effectively elevate the levels of XCT, GPX4, and GSH. This confirms that SIRT1 indeed plays

a pivotal role in regulating XCT, GPX4, and GSH metabolism during myocardial hypoxia-reoxygenation, thereby reducing the incidence of ferroptosis.

SIRT1 is a key regulator of ferroptosis. AMP-activated protein kinase (AMPK) is an important energy sensor and a master regulator of cellular metabolism, which is associated with many pathological conditions, including cardiovascular diseases.<sup>21</sup> It is a classical downstream molecule of SIRT1. Previous studies have demonstrated that trifluoperazine can attenuate rat ferroptosis-related cerebral ischemia-reperfusion injury through AMPK/FoxO3a/SLC7A11 signaling and mitochondrial-dependent mechanism.<sup>22</sup> The increase of AMPK activity during ischemia can preserve energy homeostasis and promote cell survival, which is essential for the organism stability.<sup>21</sup> In our study, the energy stress induced by oxygen-glucose deprivation elicited the phosphorylation of APMK. And the addition of bergenin further augmented the phosphorylation level of AMPK. During MIRI, the mitochondrial function of cardiomyocytes is compromised, leading to the imbalance of mitochondrial autophagy, which further results in the increase of iron droplets.<sup>17</sup>

AMPK can regulate the mitochondrial function state by activating peroxisome proliferator-activated receptor- $\gamma$  coactivator-1 $\alpha$  (PGC-1 $\alpha$ ). PGC-1 $\alpha$  is one of the main regulators of mitochondrial biogenesis. It regulates the expression of mitochondrial genes by activating several transcription factors, including nuclear respiratory factor-1 and nuclear respiratory factor-2. Bergenin can increase the expression level of PGC1- $\alpha$ , while EX527 reduces its expression.<sup>23</sup> Therefore, we propose that the protective effect of bergenin may be partly mediated by SIRT1/AMPK/PGC1- $\alpha$ .

In summary, we found that SIRT1 lowers the ferroptosis level by decreasing iron accumulation and regulating XCT/GPX4/GSH expression, and also regulates the energy metabolism during stress by SIRT1/AMPK/PGC1- $\alpha$ , improves the mitochondrial function, and diminishes the subsequent ferroptosis. SIRT1 plays a vital role in protecting the myocardium from ischemia/reperfusion injury, and its mechanism is complex and requires further investigation.

## Shortcomings and Deficiencies

We did not perform genetic knockdown of SIRT1, which could make the role of SIRT1 more definitive. We could further explore the specific mechanism by which bergenin activates sirt1 in the future. The effect of the sirt1 pathway on ferroptosis deserves to be further investigated.

## Author Contributions

All authors made a significant contribution to the work reported, whether that is in the conception, study design, execution, acquisition of data, analysis and interpretation, or in all these areas; took part in drafting, revising or critically reviewing the article; gave final approval of the version to be published; have agreed on the journal to which the article has been submitted; and agree to be accountable for all aspects of the work.

## Funding

This research received funding from Medical Science Research Project of Hebei (20240197).

## Disclosure

Lingmei Jia and Siqi Yang are co-first authors for this study. The authors declare that they have no known competing financial interests or personal relationships that could have appeared to influence the work reported in this paper.

## References

1. Tsao CW, Aday AW, Almarazooq ZI, et al. Heart disease and stroke statistics-2022 update: a report from the American Heart Association [published correction appears in *Circulation*. 2022 Sep 6;146(10):e141]. *Circulation*. 2022;145(8):e153–e639. doi:10.1161/CIR.0000000000001052
2. Dauerman HL, Ibanez B. The edge of time in acute myocardial infarction. *J Am Coll Cardiol*. 2021;77(15):1871–1874. doi:10.1016/j.jacc.2021.03.003
3. Zhang XJ, Liu X, Hu M, et al. Pharmacological inhibition of arachidonate 12-lipoxygenase ameliorates myocardial ischemia-reperfusion injury in multiple species. *Cell Metab*. 2021;33(10):2059–2075.e10. doi:10.1016/j.cmet.2021.08.014
4. Algoet M, Janssens S, Himmelreich U, et al. Myocardial ischemia-reperfusion injury and the influence of inflammation. *Trends Cardiovasc Med*. 2023;33(6):357–366. doi:10.1016/j.tcm.2022.02.005

5. Jiang X, Stockwell BR, Conrad M. Ferroptosis: mechanisms, biology and role in disease. *Nat Rev mol Cell Biol.* **2021**;22(4):266–282. doi:10.1038/s41580-020-00324-8
6. Stoyanovsky DA, Tyurina YY, Shrivastava I, et al. Iron catalysis of lipid peroxidation in ferroptosis: regulated enzymatic or random free radical reaction? *Free Radic Biol Med.* **2019**;133:153–161. doi:10.1016/j.freeradbiomed.2018.09.008
7. Chen X, Li J, Kang R, et al. Ferroptosis: machinery and regulation. *Autophagy.* **2021**;17(9):2054–2081. doi:10.1080/15548627.2020.1810918
8. Ursini F, Maiorino M. Lipid peroxidation and ferroptosis: the role of GSH and GPx4. *Free Radic Biol Med.* **2020**;152:175–185. doi:10.1016/j.freeradbiomed.2020.02.027
9. Ye Y, Chen A, Li L, et al. Repression of the antiporter SLC7A11/glutathione/glutathione peroxidase 4 axis drives ferroptosis of vascular smooth muscle cells to facilitate vascular calcification. *Kidney Int.* **2022**;102(6):1259–1275. doi:10.1016/j.kint.2022.07.034
10. Zhang T, Deng W, Deng Y, et al. Mechanisms of ferroptosis regulating oxidative stress and energy metabolism in myocardial ischemia-reperfusion injury and a novel perspective of natural plant active ingredients for its treatment. *Biomed Pharmacother.* **2023**;165:114706.
11. Fang X, Wang H, Han D, et al. Ferroptosis as a target for protection against cardiomyopathy. *Proc Natl Acad Sci.* **2019**;116(7):2672–2680. doi:10.1073/pnas.1821022116
12. Zhai Z, Zou P, Liu F, et al. Ferroptosis is a potential novel diagnostic and therapeutic target for patients with cardiomyopathy. *Front Cell Dev Biol.* **2021**;9:649045. doi:10.3389/fcell.2021.649045
13. Zhang W, Qian S, Tang B, et al. Resveratrol inhibits ferroptosis and decelerates heart failure progression via sirt1/p53 pathway activation. *J Cell Mol Med.* **2023**;27:3075–3089.
14. Salimo ZM, Yakubu MN, da Silva EL, et al. Chemistry and pharmacology of bergenin or its derivatives: a promising molecule. *Biomolecules.* **2023**;13(3):403. doi:10.3390/biom13030403
15. Yang L, Zheng Y, Miao YM, et al. Bergenin, a PPAR $\gamma$  agonist, inhibits Th17 differentiation and subsequent neutrophilic asthma by preventing GLS1-dependent glutaminolysis. *Acta Pharmacol Sin.* **2022**;43(4):963–976. doi:10.1038/s41401-021-00717-1
16. Zhang X, Zhang F, Yao F, et al. Bergenin has neuroprotective effects in mice with ischemic stroke through antioxidative stress and anti-inflammation via regulating Sirt1/FOXO3a/NF- $\kappa$ B signaling. *NeuroReport.* **2022**;33(13):549–560. doi:10.1097/WNR.0000000000001789
17. Liao Y, Ke B, Long X, et al. Abnormalities in the SIRT1-SIRT3 axis promote myocardial ischemia-reperfusion injury through ferroptosis caused by silencing the PINK1/parkin signaling pathway. *BMC Cardiovasc Disord.* **2023**;23(1):582.
18. Liu Y, Tan Y, Cao G, et al. Bergenin alleviates myocardial ischemia-reperfusion injury via SIRT1 signaling. *Biomed Pharmacother.* **2023**;158:114100. doi:10.1016/j.biopha.2022.114100
19. Yu H, Gan D, Luo Z, et al.  $\alpha$ -Ketoglutarate improves cardiac insufficiency through NAD $^{+}$ -SIRT1 signaling-mediated mitophagy and ferroptosis in pressure overload-induced mice. *Mol Med.* **2024**;30(1):15. doi:10.1186/s10020-024-00783-1
20. Ma S, Sun L, Wu W, et al. USP22 protects against myocardial ischemia-reperfusion injury via the SIRT1-p53/SLC7A11-dependent inhibition of ferroptosis-induced cardiomyocyte death. *Front Physiol.* **2020**;11. doi:10.3389/fphys.2020.551318
21. Steinberg GR, Hardie DG. New insights into activation and function of the AMPK. *Nat Rev Mol Cell Biol.* **2023**;24(4):255–272. doi:10.1038/s41580-022-00547-x
22. Zhong S, Chen W, Wang B, et al. Energy stress modulation of AMPK/FoxO3 signaling inhibits mitochondria-associated ferroptosis. *Redox Biol.* **2023**;63:102760. doi:10.1016/j.redox.2023.102760
23. Spaulding HR, Yan Z. AMPK and the adaptation to exercise. *Annu Rev Physiol.* **2022**;84(1):209–227. doi:10.1146/annurev-physiol-060721-095517
24. Salazar G, Cullen A, Huang J, et al. SQSTM1/p62 and PPARGC1A/PGC-1 $\alpha$  at the interface of autophagy and vascular senescence. *Autophagy.* **2020**;16(6):1092–1110. doi:10.1080/15548627.2019.1659612